A Neural Circuit for Acoustic Navigation combining Heterosynaptic and Non-synaptic Plasticity that learns Stable Trajectories

Danish Shaikh[1] and Poramate Manoonpong[2]

Embodied AI and Neurorobotics Laboratory (http://ens-lab.sdu.dk/)
Centre for BioRobotics, Maersk Mc-Kinney Moeller Institute, University of Southern Denmark, 5230 Odense M, Denmark
[1]danish@mmmi.sdu.dk, [2]poma@mmmi.sdu.dk

Abstract. Reactive spatial robot navigation in goal-directed tasks such as phonotaxis requires generating consistent and stable trajectories towards an acoustic target while avoiding obstacles. High-level goal-directed steering behaviour can steer a robot towards the target by mapping sound direction information to appropriate wheel velocities. However, low-level obstacle avoidance behaviour based on distance sensors may significantly alter wheel velocities and temporarily direct the robot away from the sound source, creating conflict between the two behaviours. How can such a conflict in reactive controllers be resolved in a manner that generates consistent and stable robot trajectories? We propose a neural circuit that minimises this conflict by learning sensorimotor mappings as neuronal transfer functions between the perceived sound direction and wheel velocities of a simulated non-holonomic mobile robot. These mappings constitute the high-level goal-directed steering behaviour. Sound direction information is obtained from a model of the lizard peripheral auditory system. The parameters of the transfer functions are learned via an online unsupervised correlation learning algorithm through interaction with obstacles in the form of low-level obstacle avoidance behaviour in the environment. The simulated robot is able to navigate towards a virtual sound source placed 3 m away that continuously emits a tone of frequency 2.2 kHz, while avoiding randomly placed obstacles in the environment. We demonstrate through two independent trials in simulation that in both cases the neural circuit learns consistent and stable trajectories as compared to navigation without learning.

Keywords: behaviour-based robotics, reactive navigation, phonotaxis, lizard peripheral auditory system, synaptic plasticity, correlation-based learning

1 Introduction

Navigating towards a sound source is relevant is several real-world applications. For example, mobile robots in the home that autonomously navigate to a human

speaker in response to voice commands can be useful in the human-robot interaction context. Such robots could also navigate towards people living alone that are immobilised due to injury sustained by falling down but are able to vocalise—a common problem among the elderly population. Furthermore, search-and-rescue robots looking for visually undetectable survivors amongst rubble and large debris in natural disaster scenarios such as earthquakes can use audition as a sensor modality for navigation in such cluttered environments.

Navigation is one of the earliest problems that has been investigated in the mobile robotics community. Control architectures (see [17] for a comparative review) for mobile robot navigation can be broadly classified into three types—reactive, deliberative and hybrid (a combination of deliberative and reactive). These architectures differ in the level of sensing, planning and acting performed [1]. Deliberative and hybrid control architectures can generate optimal robot trajectories but require precise a priori knowledge of the environment respectively at the global or local level. These approaches also consume significant computational power to achieve this optimality. Purely reactive controllers on the other hand are advantageous in that they do not rely on formal path planning algorithms that necessitate such precise and local/global knowledge of the environment *a priori*. Such controllers also tend to employ behaviour-based architectures [3] such as the widely known subsumption architecture [6]. The neural circuit presented here differs from the subsumption architecture in that the low-level obstacle avoidance behaviour modulates the parameters of the high-level goal-directed steering behaviour via unsupervised learning. Therefore, no explicit hand-tuning of the high-level behaviour is necessary. There has also been significant research in neurobiologically-inspired map-based navigation for mobile robots (see [24] for a review on the research in the last decade) where the focus has been on specialised neurons for spatial awareness and navigation in rodents.

Path-planning and obstacle avoidance are core components in mobile robot navigation and a number of techniques have been developed. Reviews of various approaches from different perspectives can be found in [22,13]. Path planning can be global or local, where the environment is respectively fully or locally known. Global path planning is usually performed offline due to high computational requirements while local path planning is performed online due to relatively lower computational requirements. Here we focus on online reactive path planning using only local information about the distance of the closest approaching obstacle and the direction of the target.

There are several analytical approaches in the literature on reactive acoustic navigation for mobile robots with obstacle avoidance [11,4,2,26,27,12], differing in the number of microphones as well as number and type of distance sensor(s) used. Our approach focusses on developing a purely reactive control architecture with two sound sensors and one distance sensor. This architecture is in the form of a neural circuit that implements two behaviours—high-level goal-directed steering and low-level obstacle avoidance. The neural circuit combines two brain-inspired mechanisms involved in learning and memory—heterosynaptic plasticity and non-synaptic plasticity. These two mechanisms allows a simulated non-

holonomic mobile robot to learn stable trajectories towards an acoustic target, placed 3 m away, emitting a continuous tone of 2.2 kHz. The neural circuit is validated in simulation and its performance with and without learning is compared. Sound direction information is extracted by a previously developed model of the lizard peripheral auditory system [23]. This model has been extensively studied via various robotic implementations [21]. Braitenberg sensorimotor mappings [5] between the extracted sound direction and the robot's motor velocities are used to generate the goal-directed steering behaviour (phonotaxis), while the parameters of these mappings are modulated via Input Correlation (ICO) learning [19] during the obstacle avoidance behaviour. Thus, interaction with obstacles is explicitly exploited to fine-tune parameters of the high-level behaviour and learn consistent and stable trajectories. ICO learning is unsupervised, closed-loop, correlation learning adapted from differential Hebbian learning [15,14].

This paper is organised in the following manner. Section 2 describes the lizard peripheral auditory system model and its response characteristics. Heterosynaptic and non-synaptic plasticity are also described here. Section 3 describes the neural circuit and the experimental setup. Simulation results are presented and discussed in Sect. 4. Section 5 summarises the research and outlines further work.

2 Background

2.1 Lizard peripheral auditory system

The lizard peripheral auditory system (1**A**, left) has two eardrums (TM) connected via internal air-filled Eustachian tubes (ET) opening into a central cavity. Sound passes through the ET, linking the two eardrums acoustically. This acoustical coupling maps small phase differences (corresponding to interaural time differences in the μ-sec scale) between sound waves impressing at either ear into relatively larger differences of up to 20 dB in sound amplitudes sensed at either ear. The magnitude of the phase difference and therefore the sensed amplitude difference corresponds to the relative direction from which sound arrives.

A lumped-parameter electrical model [9] (Fig. 1**A**, right) of the lizard peripheral auditory system mimics its filtering effects. Voltages V_I and V_C respectively model sound pressures P_I and P_C at the ipsilateral (towards the location of the sound source) and contralateral (away from the location of the sound source) ears. P_I and P_C respectively trigger the flow of currents i_I and i_C, that model eardrum vibrations, through impedances Z_r and Z_v. Z_r model the total acoustic filtering due to the stiffness of the ET and the eardrum mass while Z_v models the acoustic filtering effects of the central cavity. The resultant sound pressure in this cavity as modelled by voltage V_cc, due to the superposition of internal sound pressures experienced from either end triggers the flow of current i_cc. This current models the sound wave propagation inside the central cavity due to variations in the sound pressure inside it. This model generates as outputs $|i_\mathrm{I}|$ and $|i_\mathrm{C}|$ (Fig. 1**B**), which respectively are the sensed ipsilateral and contralateral amplitudes at the corresponding ear. Sound direction information is encoded into these quantities as described earlier and formulated as

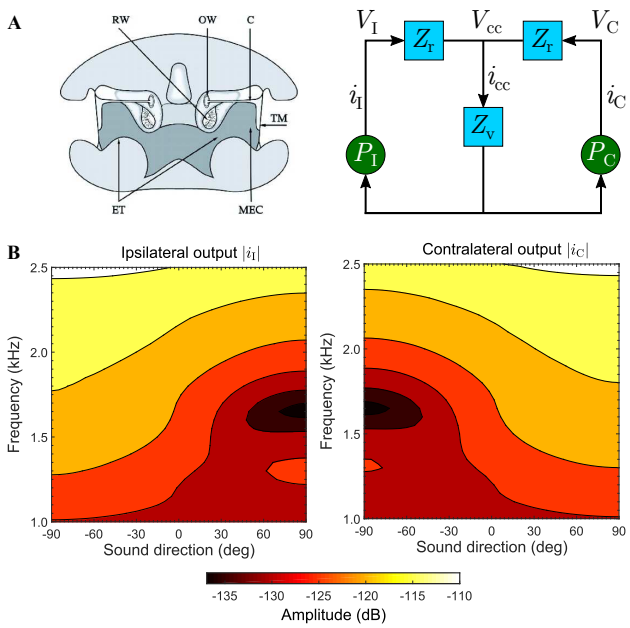

Fig. 1. Sound direction information driving phonotaxis behaviour. **A** Cross-section [7] (left) of a lizard (genus *Sceloporus*) peripheral auditory system and its electrical equivalent [9] (right). **B** The outputs $|i_I|$ (left) and $|i_C|$ (right) as given by (1).

$$\begin{aligned} |i_I| &= |G_I \cdot V_I + G_C \cdot V_C| \equiv 20 \log |i_I| \,\mathrm{dB} \text{ and} \\ |i_C| &= |G_C \cdot V_I + G_I \cdot V_C| \equiv 20 \log |i_C| \,\mathrm{dB}. \end{aligned} \tag{1}$$

G_I and G_C respectively are sound frequency-specific (1-2.2 kHz) ipsilateral and contralateral gains. These terms are experimentally derived via laser vibrometry [7] measurements of ear vibrations and are implemented as 4th-order digital infinite impulse response bandpass filters. The symmetry of the model implies that its outputs $|i_I|$ and $|i_C|$ are identical for a sound signal arriving directly from the front or the back in the azimuth plane, i.e. there is front-back ambiguity. Furthermore, when $|i_I| > |i_C|$ the sound signal coming from the ipsilateral side and when $|i_C| > |i_I|$ it is coming from the contralateral side. $|i_I|$ and $|i_C|$ vary symmetrically but non-linearly with the sound direction, respectively reaching maxima and minima towards the extremes of the relevant range of $[-90°, +90°]$.

2.2 Plasticity and learning in the biological brain

Biological neurons are interconnected via synapses, that act as a bridge between two individual neurons (see Fig. 2**A**[1]). Electrical signals are propagated

[1] modified from https://en.wikipedia.org/wiki/Nonsynaptic_plasticity#/media/File:Neurons_big1.jpg

between a pre-synaptic neuron and a post-synaptic neuron via biochemical processes occurring in these synapses. Changes in the properties of these synapses influence (but not exclusively) whether the post-synaptic neuron will fire or not in response to synaptic input from a pre-synaptic neuron. This phenomenon of activity-induced changes in the synapses is referred to as *synaptic plasticity* [20]. These changes can make the synapse relatively weaker or stronger, respectively decreasing or increasing the efficacy of the synaptic connection between the pre-synaptic and post-synaptic neuron. Synaptic plasticity is believed to be the core biochemical process underlying learning and memory.

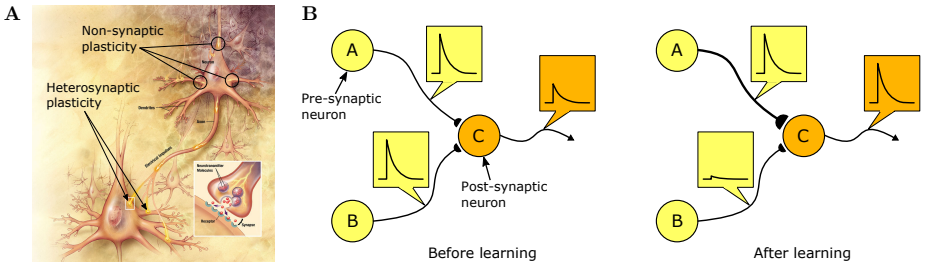

Fig. 2. Neuroplasticity and learning. **A** Illustration showing heterosynaptic and non-synaptic plasticity sites in the brain. **B** Hypothetical neural circuit before and after Input Correlation learning. During learning, temporally correlated activities of sensory neurons A and B leads to gradual increase in strength of synapse (depicted as a thick line) between A and motor neuron C. This leads to stronger activation of neuron C, causing correspondingly stronger behavioural response. After learning the behavioural response is strong enough to avoid activation of neuron B.

Change in the synaptic strength between two neurons is typically dependent on the activity of the pre-synaptic neuron. However the activity of a third neuron can releases chemical neuromodulators that induce changes in synaptic strength between two other neurons as well, a phenomenon referred to as *heterosynaptic plasticity*. The intrinsic excitability, i.e. sensitivity to synaptic input, of neurons can also be altered. This is manifested as changes in the firing characteristics of the neuron itself. Such *non-synaptic plasticity* has been observed across many species and brain areas [25]. Non-synaptic plasticity is different from synaptic plasticity in that here the neuron's properties are altered, while in the latter the properties of synapses coupling two neurons together are altered. This form of plasticity is not well understood and has been suggested as a regulation mechanism to maintain a neuron's average firing rate at a target level.

Multimodal sensory stimuli while interaction with the environment modify the structure of the brain and change the stimulus-action relationship. These stimuli strengthen or weaken synapses between neurons and allow an organism to learn new associations between sensory inputs of different modalities in an unsupervised manner. Hebbian learning [10] is considered to be one form of such unsupervised associative learning, and is theorised to be the underlying

mechanism for synaptic plasticity in the brain. One form of Hebbian-like learning is ICO learning [19], which is an online unsupervised differential Hebbian learning algorithm that implements heterosynaptic plasticity. Here, change in synaptic strength between a pre-synaptic neuron and a post-synaptic neuron is driven by the temporally correlated activity of all neurons projecting on to the post-synaptic neuron (see Fig. 2**B**). The post-synaptic neuron's output is a linear combination of all inputs, and indirectly influences the activity of both the input neurons via a defined behavioural response. ICO learning produces a behavioural response that nullifies the activation of the input neuron whose response temporally lags that of the other input neuron. ICO learning is fast, stable and can successfully generate adaptive behaviour in real robots [18,16].

3 Materials and methods

The simulated mobile robot is modelled as a differential drive robot with two wheels (see Fig. 3), which imposes non-holonomic kinematic constraints. The distance l between the centres of the two wheels is defined to be 16 cm. The robot has two virtual acoustic sensors that functionally mimic microphones and receive auditory signals from the acoustic target towards which the robot must navigate. The separation d between these sensors is 13 mm because the parameters of the lizard peripheral auditory model have been derived from an animal with a 13 mm separation between its ear. The acoustic sensor separation must match that value, otherwise the actual ITD cue and the ITD cues to which the peripheral auditory model is tuned will be unmatched. These auditory signals are processed by the lizard peripheral auditory model and its outputs are fed as inputs to the neural circuit described next. Phonotaxis is performed exclusively via these auditory signals. The robot also has a distance sensor located at its centre that provides as outputs the distance of obstacles from the robot, within a 180° field-of-view in front of the robot, and its relative location. This sensor functionally mimics a laser range finder, a common distance sensor used in mobile robots for navigation purposes. White Gaussian noise at 20 dB and 3 dB is respectively added to the auditory inputs and to the distance sensor input to simulate noisy sensors. The forward kinematic model for differential drive mobile robots [8] as given by (2) is used to determine the pose $[x, y, \theta]$ of the robot, where (x, y) are the two-dimensional coordinates and θ is the heading.

$$\begin{bmatrix} x \\ y \\ \theta \end{bmatrix} = \begin{bmatrix} cos(\omega\delta t) & -sin(\omega\delta t) & 0 \\ sin(\omega\delta t) & cos(\omega\delta t) & 0 \\ 0 & 0 & 1 \end{bmatrix} \begin{bmatrix} Dsin(\theta) \\ -Dcos(\theta) \\ \theta \end{bmatrix} + \begin{bmatrix} x - Dsin(\theta) \\ y + Dcos(\theta) \\ \omega\delta \end{bmatrix}$$
$$\text{where, angular velocity } \omega = \frac{(v_r - v_l)}{l} \text{ and,} \tag{2}$$
$$\text{distance } D \text{ from instantaneous center of curvature} = \frac{l}{2}\frac{(v_r + v_l)}{(v_r - v_l)} \ .$$

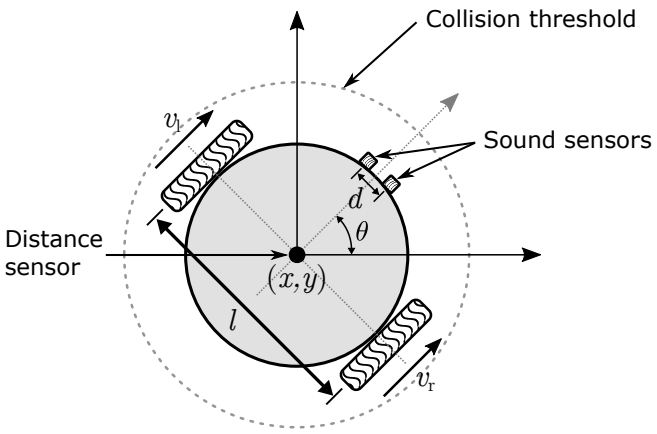

Fig. 3. Mobile robot kinematics.

Figure 4 depicts the neural circuit for reactive navigation with obstacle avoidance. The Braitenberg sensorimotor cross-couplings implement a mapping between the auditory inputs (sound direction information in decibels coming from the lizard peripheral auditory system) and the motor outputs (linear wheel velocities in cm/s). The sensorimotor couplings are defined such that the ipsilateral auditory input proportionally drives the contralateral motor output. The robot respectively turns either left or right, based on whether the left auditory signal is greater than the right auditory signal ($|i_\mathrm{I}| > |i_\mathrm{C}|$) or vice versa ($|i_\mathrm{C}| > |i_\mathrm{I}|$). The radius of the turn is proportional to the relative magnitudes of the auditory signals. When the robot is directly facing the target, the two acoustic sensors are equidistant from the target. In this condition there is no phase difference between the auditory signals arriving at the two acoustic sensors and thus the peripheral auditory model's outputs are identical. Therefore the wheel velocities are also identical, resulting in the robot moving in a straight line. These sensorimotor cross-couplings, implemented as micro-circuits with two sensorimotor neurons having non-linear sigmoid transfer functions, generate phonotaxis behaviour. The two transfer functions are respectively defined as

$$v_\mathrm{l} = \frac{4}{1+\beta_\mathrm{r} e^{-|i_\mathrm{C}|}} \text{ and} v_\mathrm{r} = \frac{4}{1+\beta_\mathrm{l} e^{-|i_\mathrm{I}|}} \tag{3}$$

where the parameters β_l and β_r determine the amount of respective horizontal shifts. The transfer functions have finite limits between 0 cm/s to 4 cm/s. The strengths of these couplings are determined by the intrinsic excitability of the individual sensorimotor neurons, which is modelled as the horizontal shift in the transfer functions. The two identical micro-circuits that implement ICO learning modify β_l and β_r and shift these transfer functions during learning.

The micro-circuits implementing obstacle avoidance behaviour respectively inhibit and excite the ipsilateral and contralateral outputs of the sensorimotor neurons. If the closest approaching obstacle is detected to be within the collision

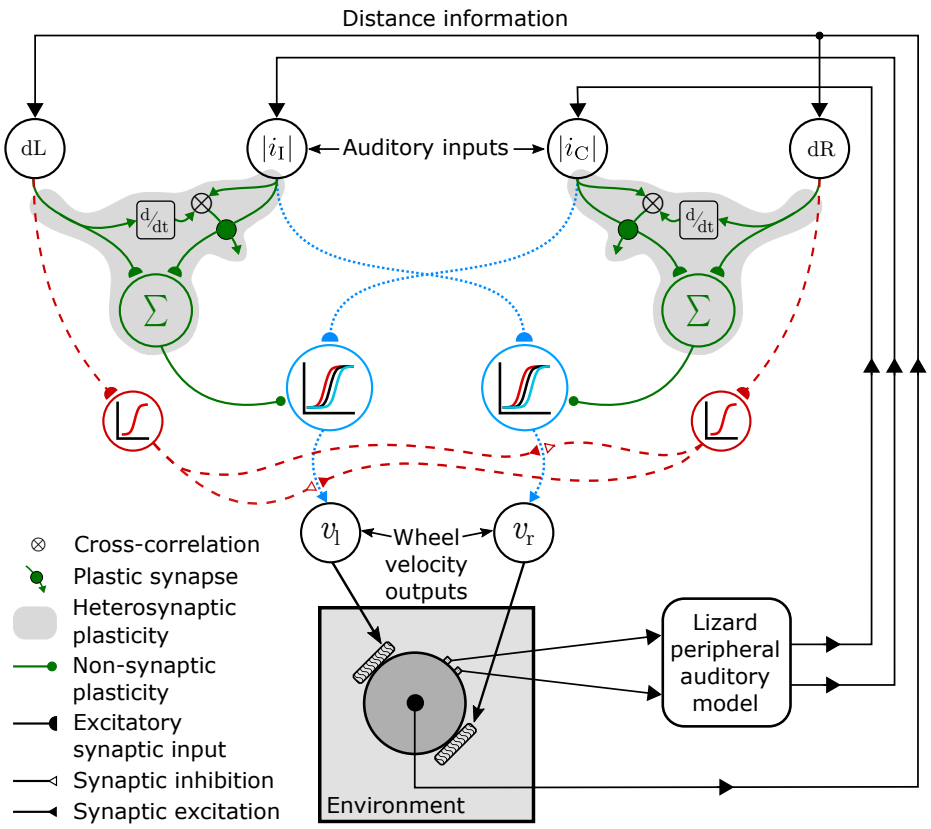

Fig. 4. The neural circuit for reactive navigation with obstacle avoidance embodied in the environment. The sensorimotor mappings between the auditory inputs $|i_I|$ and $|i_C|$ and the motor outputs v_l and v_r (dotted blue lines) implement phonotaxis behaviour. The micro-circuits implementing ICO learning (solid lines inside the shaded areas) modify the strengths, modelled by β_l and β_r, of these mappings. The obstacle avoidance behaviour is implemented by the sensorimotor mappings, with fixed strengths, between the distance sensor inputs and motor outputs (dashed red lines).

threshold, a obstacle avoidance reflex is triggered that makes the robot turn sharply away from the obstacle. This reflex is implemented by enhancing the motor velocity output to the wheel on the same side as the obstacle to a relatively high but fixed value of 4 cm/s while the motor velocity output to the opposite wheel is suppressed to a relatively low but fixed value of 0.1 cm/s. This causes the robot to sharply turn left when it detects an obstacle to its right and vice versa. The collision threshold (see Fig. 3) is the perimeter of radius 20 cm, centred on the robot. The navigation goal is to move towards an acoustic target located 3 m away from the initial position of the robot, while avoiding any obstacles in the environment. Since the strength of the Braitenberg couplings determines the

straightness of the robot's trajectories, the ICO learning algorithm must learn the best possible coupling that generates as straight trajectories as possible.

The initial pose of the robot is set to $[0, 0, 0°]$. A random number of circular obstacles are randomly distributed in the environment between the robot and the target as well as around the target. The size of the obstacles are randomly chosen but are below a threshold equal to the wavelength of the sinusoidal acoustic signal of frequency 2.2 kHz emitted by the target. This threshold is calculated as $\frac{\text{speed of sound in air in cm/s}}{\text{sound frequency in Hz}} = \frac{34000}{2200} = 15.45\,\text{cm}$. Wheel slip is not modelled to maintain relative simplicity.

The learning is performed for a maximum of 50 iterations to keep simulation time reasonable. The learning is stopped either when the robot reaches the acoustic target without triggering the obstacle avoidance behaviour or when all 50 iterations are complete. Each iteration runs for a maximum of 1000 time steps. At each simulation time step of 1 s, the sound direction information is extracted and wheel velocities are computed via the sigmoid transfer functions. Then the new pose of the robot based on current wheel velocities is determined by (2). If the robot encounters an obstacle within its collision threshold, the obstacle avoidance reflex overrides the calculated wheel velocities as described earlier. The obstacle avoidance reflex lasts as long as the obstacle remains inside the collision threshold. At each time step during the obstacle avoidance maneuver, ICO learning respectively updates the parameters β_l and β_r using the temporal correlation between the ipsilateral and contralateral auditory signal and the distance sensor signal. β_l and β_r are initialised to random values between 0 and 1, while synaptic weights w_l and w_r are initialised to random values between 0 and 0.1. The learning rate η is set to 0.01. β_l and β_r are updated as

$$\begin{aligned} \frac{\delta \beta_\text{l}}{\delta t} &= w_\text{l} \left| i_\text{I} \right| + \text{dL} \ \text{, where } \frac{\delta w_\text{l}}{\delta t} = \eta \left| i_\text{I} \right| \frac{\delta \text{dL}}{\delta t} \ \text{, and} \\ \frac{\delta \beta_\text{r}}{\delta t} &= w_\text{r} \left| i_\text{C} \right| + \text{dR} \ \text{, where } \frac{\delta w_\text{r}}{\delta t} = \eta \left| i_\text{C} \right| \frac{\delta \text{dR}}{\delta t} \ . \end{aligned} \tag{4}$$

Since (4) is simply positive feedback, allowing the ICO learning algorithm to run without restraint will cause β_l and β_r to increase uncontrollably. This will continuously push the transfer function curves to the right such that the both v_l and v_r, and thus the robot's linear velocity, will eventually become infinitesimally small. To counter this, β_l and β_r are exponentially decreased as function of time during learning. This is done by multiplying β_l and β_r with an time varying scaling factor defined as $e^{(-t/\text{k})}$, where t is the current time step and k is chosen via trial-and-error to be 60000. This negative feedback prevents the uncontrollable shift in the transfer functions and maintains homeostasis.

4 Results and discussion

Figure 5 depicts the performance of the neural circuit in two independent trials. When the learning is not used, the neural circuit produces more winding

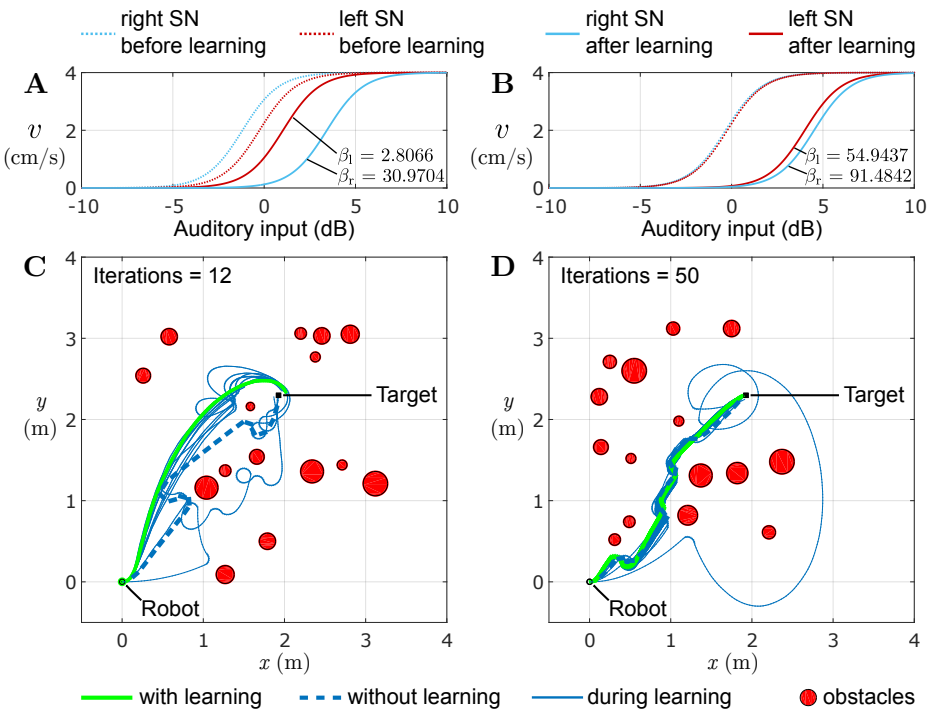

Fig. 5. Acoustic navigation with the proposed neural circuit. **A and B** The transfer functions of the left SN (red) and right SN (blue) before learning (dotted) and after learning (solid). **C and D** Robot trajectories without learning (dotted), during learning (solid blue) and after learning (solid green).

trajectories as compared to when using learning. In this case the robot always attempts to move in a straight line towards the target due to the strong and constant Braitenberg sensorimotor couplings between the auditory inputs and the motor outputs. This straight trajectory is heavily modified by the obstacle avoidance behaviour such that robot makes sharp turns while avoiding obstacles and reorienting towards the target. When learning is enabled, the neural circuit learns relatively smoother trajectories. The robot is able to either completely suppress its obstacle avoidance behaviour (Fig. 5, **A** and **C**) or minimise it to a relatively large extent (Fig. 5, **B** and **D**). This is due to the modification of the strengths of the sensorimotor couplings by the ICO learning algorithm during interaction with the obstacles. The neural circuit tries to learn the best possible sensorimotor couplings that minimise sharp turns during movement. Early in the learning process the robot generates very winding trajectories, since the Braitenberg sensorimotor couplings are initially relatively weak. This enforces circular trajectories with the turning radius being dependent on the strength of the couplings. As the learning progresses, the sensorimotor couplings adapt to the environment and the robot moves in progressively straighter trajectories.

5 Conclusions and future directions

We have presented a neural circuit for reactive acoustic navigation with obstacle avoidance. The circuit uses simple Braitenberg acoustomotor couplings to realise goal-directed navigation behaviour towards an acoustic target located 3 m away, emitting a continuous 2.2 kHz tone. The strength of these couplings are learned through interaction with obstacles in the environment, realised as obstacle avoidance behaviour. The circuit learns stable and consistent trajectories using only noisy sensor information about sound direction, extracted via a model of the lizard peripheral auditory system, and distance from closest obstacle. In this manner the low-level obstacle avoidance behaviour modifies the high-level goal-directed steering behaviour to resolve the conflicting trajectories that these behaviours enforce. The circuit allowed a simulated mobile robot to follow relatively smooth trajectories during phonotaxis while avoiding obstacles. In comparison, trajectories generated without learning were relatively less smooth. The immediate next steps are to validate the neural circuit in real robot trials.

The trajectories generated by the proposed neural circuit are sub-optimal and characteristic of reactive navigation. Strong Braitenberg couplings tend to enforce straight-line trajectories that are difficult to maintain in cluttered environments. Smoother trajectories may be obtained by correcting them pre-emptively to circumvent the obstacle avoidance behaviour. ICO learning can be used to modify the sensorimotor couplings for obstacle avoidance behaviour so that the robot turns progressively earlier in time in response to approaching obstacles.

6 Acknowledgements

This research was supported with a grant for the SMOOTH project (project number 6158-00009B) by Innovation Fund Denmark.

References

1. Alves, S., Rosario, J., Ferasoli Filho, H., Rincon, L., Yamasaki, R.: Conceptual bases of robot navigation modeling, control and applications. In: Barrera, A. (ed.) Advances in Robot Navigation. InTech (2011)
2. Andersson, S., Shah, V., Handzel, A., Krishnaprasad, P.: Robot phonotaxis with dynamic sound source localization. In: Robotics and Automation, 2004. Proceedings. ICRA '04. 2004 IEEE International Conference on. vol. 5, pp. 4833–4838 (April 2004)
3. Arkin, R.: Behavior-based robotics. MIT Press (1998)
4. Bicho, E., Mallet, P., Schner, G.: Target Representation on an Autonomous Vehicle with Low-Level Sensors. The International Journal of Robotics Research 19(5), 424–447 (2000)
5. Braitenberg, V.: Vehicles: Experiments in Synthetic Psychology. MIT Press, Bradford Books, Cambridge (1984)

6. Brooks, R.: A robust layered control system for a mobile robot. IEEE Journal on Robotics and Automation 2(1), 14–23 (Mar 1986)
7. Christensen-Dalsgaard, J., Manley, G.: Directionality of the Lizard Ear. Journal of Experimental Biology 208(6), 1209–1217 (2005)
8. Dudek, G., Jenkin, M.: Computational Principles of Mobile Robotics. Cambridge University Press, New York, NY, USA, 2 edn. (2010)
9. Fletcher, N., Thwaites, S.: Physical Models for the Analysis of Acoustical Systems in Biology. Quarterly Reviews of Biophysics 12(1), 25–65 (1979)
10. Hebb, D.: The organization of behavior: A neuropsychological theory. Psychology Press (2005)
11. Huang, J., Supaongprapa, T., Terakura, I., Wang, F., Ohnishi, N., Sugie, N.: A model-based sound localization system and its application to robot navigation. Robotics and Autonomous Systems 27(4), 199–209 (1999)
12. Hwang, B.Y., Park, S.H., Han, J.H., Kim, M.G., Lee, J.M.: Sound-Source Tracking and Obstacle Avoidance System for the Mobile Robot, pp. 181–192. Springer International Publishing, Cham (2014)
13. Janis, A., Bade, A.: Path Planning Algorithm in Complex Environment: A Survey. Transactions on Science and Technology 3(1), 31–40 (2016)
14. Klopf, A.: A neuronal model of classical conditioning. Psychobiology 16(2), 85–125 (1988)
15. Kosko, B.: Differential Hebbian learning. AIP Conference Proceedings 151(1), 277–282 (1986)
16. Manoonpong, P., Wörgötter, F.: Neural Information Processing: 16th International Conference, ICONIP 2009, Bangkok, Thailand, December 1-5, 2009, Proceedings, Part II, chap. Adaptive Sensor-Driven Neural Control for Learning in Walking Machines, pp. 47–55. Springer Berlin Heidelberg (2009)
17. Nakhaeinia, D., Tang, S., Noor, S., Motlagh, O.: A review of control architectures for autonomous navigation of mobile robots. International Journal of Physical Sciences 6(2), 169–174 (2011)
18. P., B., Wörgötter, F.: Fast heterosynaptic learning in a robot food retrieval task inspired by the limbic system. Biosystems 89(1-3), 294–299 (2007), selected Papers presented at the 6th International Workshop on Neural Coding
19. Porr, B., Wörgötter, F.: Strongly improved stability and faster convergence of temporal sequence learning by utilising input correlations only. Neural Computation 18(6), 1380–1412 (2006)
20. Purves, D., Augustine, G., Fitzpatrick, D., Hall, W., LaMantia, A., White, L.: Synaptic Plasticity. In: Neuroscience, pp. 163–182. Sinauer Associates, Sunderland, Massachusetts, 5 edn. (2012)
21. Shaikh, D., Hallam, J., Christensen-Dalsgaard, J.: From "ear" to there: a review of biorobotic models of auditory processing in lizards. Biological Cybernetics 110(4), 303–317 (2016)
22. Tang, S., Kamil, F., Khaksar, W., Zulkifli, N., Ahmad, S.: Robotic motion planning in unknown dynamic environments: Existing approaches and challenges. In: 2015 IEEE International Symposium on Robotics and Intelligent Sensors (IRIS). pp. 288–294 (Oct 2015)
23. Wever, E.: The Reptile Ear: Its Structure and Function. Princeton University Press (1978)
24. Zeno, P., Patel, S., Sobh, T.: Review of Neurobiologically Based Mobile Robot Navigation System Research Performed Since 2000. Journal of Robotics 2016 (2016)

25. Zhang, W., Linden, D.: The other side of the engram: experience-driven changes in neuronal intrinsic excitability. Nature Reviews Neuroscience 4(11), 885–900 (Nov 2003)
26. Zu, L., Yang, P., Zhang, Y., Chen, L., Sun, H.: Study on navigation system of mobile robot based on auditory localization. In: 2009 IEEE International Conference on Robotics and Biomimetics (ROBIO). pp. 321–326 (Dec 2009)
27. Zuojun, L., Guangyao, L., Peng, Y., Feng, L., Chu, C.: Behavior based rescue robot audio navigation and obstacle avoidance. In: Proceedings of the 31st Chinese Control Conference. pp. 4847–4851 (July 2012)